ASR488, a novel small molecule, activates an mRNA binding protein, CPEB1, and inhibits the growth of bladder cancer

ASHISH TYAGI[1], VENKATESH KOLLURU[1], BALAJI CHANDRASEKARAN[1], UTTARA SARAN[1], ARUN K. SHARMA[2], MURALI K. ANKEM[1] and CHENDIL DAMODARAN[1]

[1]Department of Urology, University of Louisville, Louisville, KY 40202; [2]Department of Pharmacology, Penn State Cancer Institute, Penn State College of Medicine, Hershey, PA 17033, USA

Received October 21, 2019; Accepted March 2, 2020

DOI: 10.3892/ol.2020.11593

Abstract. Due to a lack of mechanistic insights, muscle-invasive bladder cancer (MIBC) remains incurable and is one of the most lethal types of cancer in the United States. The present study investigated changes in the molecular signatures of MIBC cells (TCCSUP and HT1376) after treatment with a novel small molecule, ASR488, to gain knowledge of the mechanisms that inhibited MIBC cell growth. ASR488 treatment initiated apoptotic signaling in MIBC cells. Pathway enrichment analysis was used to analyze the changes in function of differentially expressed genes. Gene Ontology analysis, as well as Kyoto Encyclopedia of Genes and Genomes analysis, was also performed. These analyses along with reactome pathway enrichment analyses indicated that the genes upregulated in the ASR488-treated cells are involved in focal adhesion, neurotrophin signaling, p53 signaling, endoplasmic reticulum functioning in terms of protein processing, and pathways related to bladder cancer. The genes downregulated in ASR488-treated MIBC cells were mainly involved in DNA replication, mismatch repair, RNA degradation, nucleotide excision repair and TGFβ signaling ($P<0.05$). Furthermore, reverse transcription-quantitative PCR analysis revealed an increase in transcripts of the most upregulated genes in ASR 488-treated MIBC cells: *CPEB1* (36-fold), *IL11* (30-fold), *SFN* (20.12-fold) and *CYP4F11* (15.8-fold). In conclusion, the analysis of biological functions of the most differentially expressed genes revealed possible mechanisms that may be associated with the aggressiveness of MIBC.

Introduction

Bladder cancer (BCa) is one of the major causes of cancer related morbidity in the US and worldwide (1). In 2019, around 80,270 new cases of BCa were expected, and 17,670 estimated BCa patient deaths in the US (2). Most cases of BCa are non-muscle invasive and transurethral resection is commonly performed but with a high recurrence rate (3). However, nearly 25% of newly diagnosed BCa patients have muscle invasive bladder cancer (MIBC), and approximately half of the patients with MIBC recurrence eventually die from BCa because of the lack of treatment options (4,5). Radical cystectomy followed with pelvic lymphadenectomy is the gold standard treatment for MIBC (6). Bladder preserving trimodal therapies are also evolving as an effective alternate (7), however, combined with current platinum-based chemotherapy (such as MVAC-methotrexate, vinblastine, adriamycin, and cisplatin), 25-30% patients still require salvage cystectomy (8). The high morbidity of definitive therapy for BCa along with poor prognosis of advanced BCa warrants identification of novel targets and subsequent therapeutic interventions to achieve complete remission of BCa.

To overcome the disadvantages of traditional chemotherapy and radiotherapy, the research paradigm has shifted towards elimination of cancer cells specifically by targeting specific molecular targets. To achieve this for use in clinical practice, the current preferred approaches are search for novel and targeted small-molecule agents (9) and monoclonal antibodies (mAbs) (10). mAbs are usually large molecular weight proteins (~150 kDa), whereas small molecule cancer drugs can transfer through the plasma membranes owing to their much smaller in size (≤500 Da) (11). The cost-effectiveness and their amenable nature to oral administration make them a better choice than mAbs, which are mostly administered intravenously (12).

Small molecules are being extensively used to target oncogenic pathways that are aberrantly activated in most cancers. These molecules function by targeting the kinases that include receptors as well as their downstream regulators thus inhibiting cancer cell survival and proliferation (13,14). A better understanding of oncogenic mechanisms, as well as identification of specific genes/proteins may help design novel strategies to not only improve the efficacy of current drugs but can also be a major aid in the identification of novel agents. Advancement of systems biology can help us analyze and identify interactions between important gene networks that can provide us significant insight into biological pathways (15). The genetic processes are very complex, and these interactions

Correspondence to: Professor Chendil Damodaran, Department of Urology, University of Louisville, 505 S Hancock Street, CTR Bldg, Louisville, KY 40202, USA
E-mail: chendil.damodaran@louisville.edu

Key words: small molecules, muscle invasive bladder cancer, CPEB1, differential gene expression, apoptosis

change significantly when a cancer cell is treated with a small molecule.

Based on the structure-activity relationship studies focused on the Withaferin A (a dietary compound which exhibits anti-cancer effect against many cancer types) (16-22) analogs designed in our laboratory, we have identified a novel small molecule, ASR488, designed by protecting-OH group at 4-position of Withaferin A by thiophene-2-carbonyl functionality. ASR-488 demonstrated cell growth arrest in BCa cells and, more importantly, is non-toxic to normal BCa cells. In the current study, differential gene network analysis was performed to detect the changes in gene expression in ASR488 treated MIBC cells. Also, functional annotation and network analyses were performed to identify differential gene expression (DEGs). By analyzing the biological functions and networks of ASR488-treated MIBC cells, our findings will help to gain a better understanding of the effect of small molecules and to explore the candidate BCa treatments.

Materials and methods

Synthesis of ASR488. ASR488 was synthesized starting from Withaferin A according to a synthetic strategy recently developed in our laboratory (manuscript under preparation). Briefly, to a mixture of Withaferin A and trimethylamine in methylene chloride at 0˚C was added 2-thiophenecarbonyl chloride and the resulting reaction mixture was stirred overnight at room temperature. The reaction mixture was quenched with saturated $NaHCO_3$ solution, extracted with methylene chloride, and purified by column chromatography. The compound was characterized by NMR and MS and its purity (≥98%) was determined by HPLC.

Cell culture and viability assay. BCa cell lines TCCSUP (ATCC® HTB5™), and HT1376 (ATCC® CRL-1472™) were purchased from ATCC. Cell lines were maintained in Eagle's Minimum Essential Medium at 37˚C and 5% CO_2 (16). The anti-proliferative effect of ASR488 was determined by the MTT (3-[4,5-dimethylthiazol-2-yl]-2,5-diphenyltetrazolium bromide) assay. TCCSUP and HT1376 cells were treated with varying concentrations of ASR488 (0.2-12.5 μM) for 24, 48 and 72 h.

Detection of apoptosis by flow cytometry and immunoblotting. Annexin V-fluorescein isothiocyanate (FITC) against propidium iodide (PI) assay (FITC Annexin V Apoptosis Detection Kit I, BD Pharminogen) was used for detecting apoptosis as described previously (17). Total protein extracts from TCCSUP cells were prepared with the Mammalian Protein Extraction Reagent (Thermo Scientific) according to the manufacturer's instructions. Western blotting was performed using specific antibodies against Cleaved PARP (cat. no. 5625), BAX (cat. no. 5023), , Bcl-2 (cat. no. 4223), p65 (cat. no. 8242) (Cell signaling Technology), and β-actin (Santa Cruz Biotechnologies). The positive bands were detected using enhanced chemiluminescence.

RNA isolation, cDNA library construction, and DNA sequencing. TCCSUP cells treated with vehicle (DMSO) or ASR488 were subjected to RNA isolation using TRIzol® (Invitrogen; Thermo Fisher Scientific, Inc.) according to the manufacturer's protocol. Nano Photometer® spectrophotometer (Implen, Inc.) was used to measure the RNA concentration and purity of the samples. A cDNA library was then constructed using an NEB Next® Ultra™ RNA Library Prep kit for Illumina® (New England Biolabs, Inc.) by Novogene Bioinformatics Technologies Co. Ltd., following the manufacturer's protocols. Subsequently, polymerase chain reaction (PCR) was, Universal PCR primers, and Index (X) Primer for double-stranded cDNA amplification. The PCR products generated for PCR performed using Phusion High-Fidelity DNA polymerase were purified using the AMPure XP system, and Agilent Bioanalyzer 2100 system was used to analyze the library quality. The cDNA library was sequenced using an Illumina Hiseq 2000/2500 platform and 100 bp/50 bp single-end reads were generated.

Data analysis. Bioinformatics analysis was performed using a combination of programs including STAR, HTseq, Cufflink, and our wrapped scripts. Tophat program was used to parse the alignments and DESeq2/edgeR was utilized to ascertain differential expressions. To determine GO and KEGG enrichment Cluster Profiler was used.

Clustering. Fragments Per Kilobase of transcript per Million mapped reads (FPKM) expression level was used to cluster different samples to identify the correlation between differences. To analyze the difference between DEGs and the correlation, hierarchical clustering distance method was used with default parameters in R with the function of the heatmap, SOM (Self-organization mapping), and k means using silhouette coefficient.

GO and KEGG enrichment analysis of differentially expressed genes. Cluster profiler R package with corrected gene length bias was used for analyzing GO enrichment of DEGs. $P<0.05$ were considered significantly enriched by DEGs. Cluster profiler R package was also used to examine the statistical enrichment of differential expression genes in KEGG pathways for understanding functions as well as molecular level information of the dataset generated by the RNASeq.

Differential expression analysis

For DESeq2 with biological replicates. DESeq2 R package (2_1.6.3) was used to analyze differential expression between the ASR488 treated and control groups (two biological replicates per condition). The P-values obtained from the analysis were adjusted using the Benjamini and Hochberg's approach so that the false discovery rate (FDR) can be controlled. The genes having adjusted P-value <0.05 were assigned as differentially expressed.

For edge R without biological replicates. EdgeR program package (3.16.5) was used to adjust the read counts for each sequenced library before differential gene expression analysis, through one scaling normalized factor. The P-values were adjusted using the Benjamini and Hochberg method. A corrected P-value of 0.05 and absolute fold-change of 1 were set as the thresholds for significantly differential expression. The Venn diagrams were prepared using the function Venn diagram in R based on the gene list for different groups.

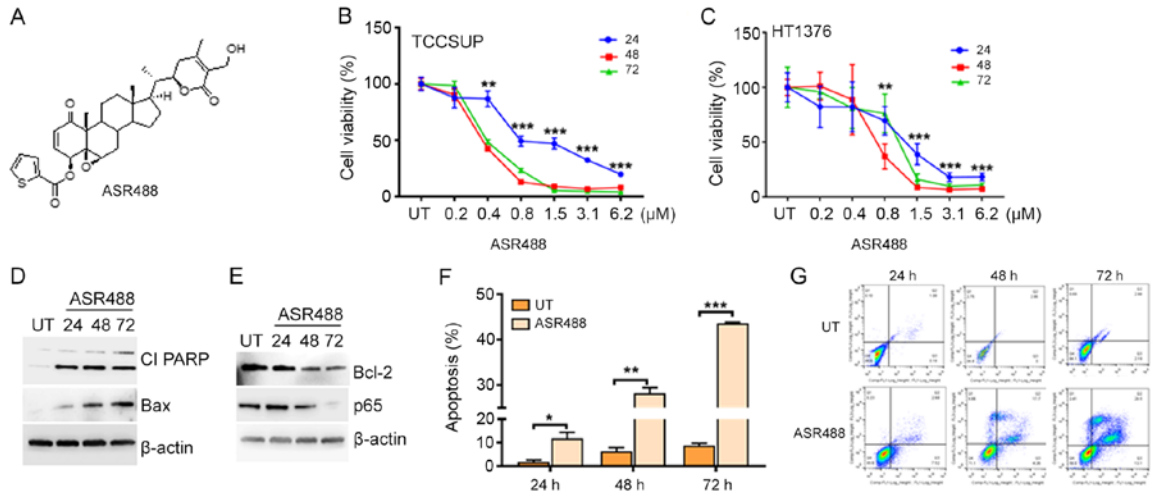

Figure 1. ASR488 treatment inhibits the growth of MIBC. (A) Structure of ASR488. (B) TCCSUP and (C) HT1376 cells were treated with the indicated concentration of ASR488 or vehicle (DMSO; UT cells) for 24, 48 and 72 h, followed by an MTT assay to assess cell viability. (D) ASR488-treated cells exhibited upregulation of the levels of cleaved PARP and Bax in a time-dependent manner. (E) ASR488-treated cells exhibited downregulation of the levels of Bcl2 and P65 in a time-dependent manner. (F) Apoptosis was quantified using flow cytometry of Annexin V-FITC and propidium iodide-stained, ASR488-treated TCCSUP cells. (G) Representative figures of FACS analysis of Annexin V-FITC and PI-stained, ASR488-treated TCCSUP cells. Student's t-test was used to identify statistically significant differences between vehicle and treatment at each concentration. *P<0.05, **P<0.01 and ***P<0.001 vs. UT. MIBC, muscle-invasive bladder cancer; Cl, cleaved; UT, vehicle (DMSO) treated TCCSUP cells.

Statistical analysis. The data are presented as the mean ± SD. The significance of the differences between the groups was determined using the unpaired Student's t-test or multiple comparisons between groups were performed using a one-way ANOVA with a post hoc Dunnett's test. P<0.05 was considered to indicate a statistically significant difference. All of the statistical analyses were performed using Prism 6 software (GraphPad Software Inc.).

Results

ASR488 treatment inhibits MIBC cell growth. To determine the therapeutic potency of ASR488 (Fig. 1A) on MIBC, we examined the effect of ASR488 treatment on cell viability of TCCSUP and HT1376 cells using the MTT assay. Significant reductions in cell viability were observed in both TCCSUP (IC_{50} at 800, 480 and 450 nM at 24, 48 and 72 h, respectively) and HT1376 (IC_{50} at 1.28 μM, 750 and 850 nM at 24, 48 and 72 h, respectively) cell lines (Fig. 1B and C). Induction of apoptosis could be interpreted by observation of increased expression of BAX and Cleaved PARP (Fig. 1D). ASR488 treatment inhibited survival signaling such as downregulation of p65 and Bcl-2 expression in ASR488 treated MIBC cell lines (Fig. 1E). Annexin V-FITC staining further corroborated the results by showing significant increases in apoptosis in both cell lines (TCCSUP: 30.5%, P=0.0382 and HT1376: 23.2%, P=0.0131) after 24 h treatment of ASR488 (Fig. 1F and G). Overall, these results suggest that ASR488 effectively initiated apoptotic signaling, which resulted in significant growth inhibition of MIBC cells.

Identification of differentially expressed genes in ASR488-treated TCCSUP cells. To identify whether there is a significant change in expression of key regulatory genes in ASR488 treated cells, we performed and analyzed RNASeq data for DEGs in ASR488-treated and vehicle-treated TCCSUP cells. A volcano map demonstrated the overall distribution of DEGs between control and ASR488-treated BCa cells. The genes presented as red dots are the upregulated genes, whereas the downregulated genes are represented as green dots, and blue dots represent the genes that remained unchanged (Fig. 2A). Our current study obtained 3770 genes that were differentially expressed in TCCSUP cells upon ASR488 treatment, of which 2,136 genes were upregulated, and 1634 were downregulated (Fig. 2A). Lists of the ten most upregulated and downregulated genes in ASR488-treated MIBC cells are given in Tables I and II. Specifically, expression levels of *CPEB1*, *ACTG2*, *SFN*, *HSPA6*, *CYP4F11*, *TAGLN*, *LINC00707*, *IL11*, *MAP1A*, *SPHK1*, and *GNGT2* were upregulated in treated TCCSUP cells, whereas expression levels of *SFRP4*, *DDX60*, *GBP4*, *BBOX1*, *RSAD2*, *OASL*, *FOS*, *IFIT2*, *CMPK2*, *STEAP4*, and *IFI44L* were the downregulated. The top five upregulated genes were confirmed by reverse transcription-quantitative PCR analysis: *CPEB1* (36-fold), *IL11* (30-fold), *SFN* (20.12-fold) and *CYP4F11* (15.8-fold) (Fig. 2D, primer details: Table SI), while no significant change was observed in downregulated genes. The top two upregulated genes CPEB1 and IL11 expressions were confirmed by immunoblotting (Fig. 2C). To identify significant DEGs during ASR488 treatment, the expression quantity of each gene in untreated and ASR488-treated TCCSUP cells was also compared pairwise and filtered with [$\log_2$(fold-change)]>1 and q value <0.005. 13,474 DEGs were detected in both datasets (Fig. 2B). Among these, 12,364 genes showed significantly differential expression in both groups. Three-hundred-forty-two genes in the ASR488 treated cells and 768 genes in the control cells showed significantly differential expression (Fig. 2B). To visualize the similarities between the two groups and also to determine if the expression profile of ASR488-treated TCCSUP cells and control cells are different, the genes that were differentially expressed in pairwise comparison were clustered. The

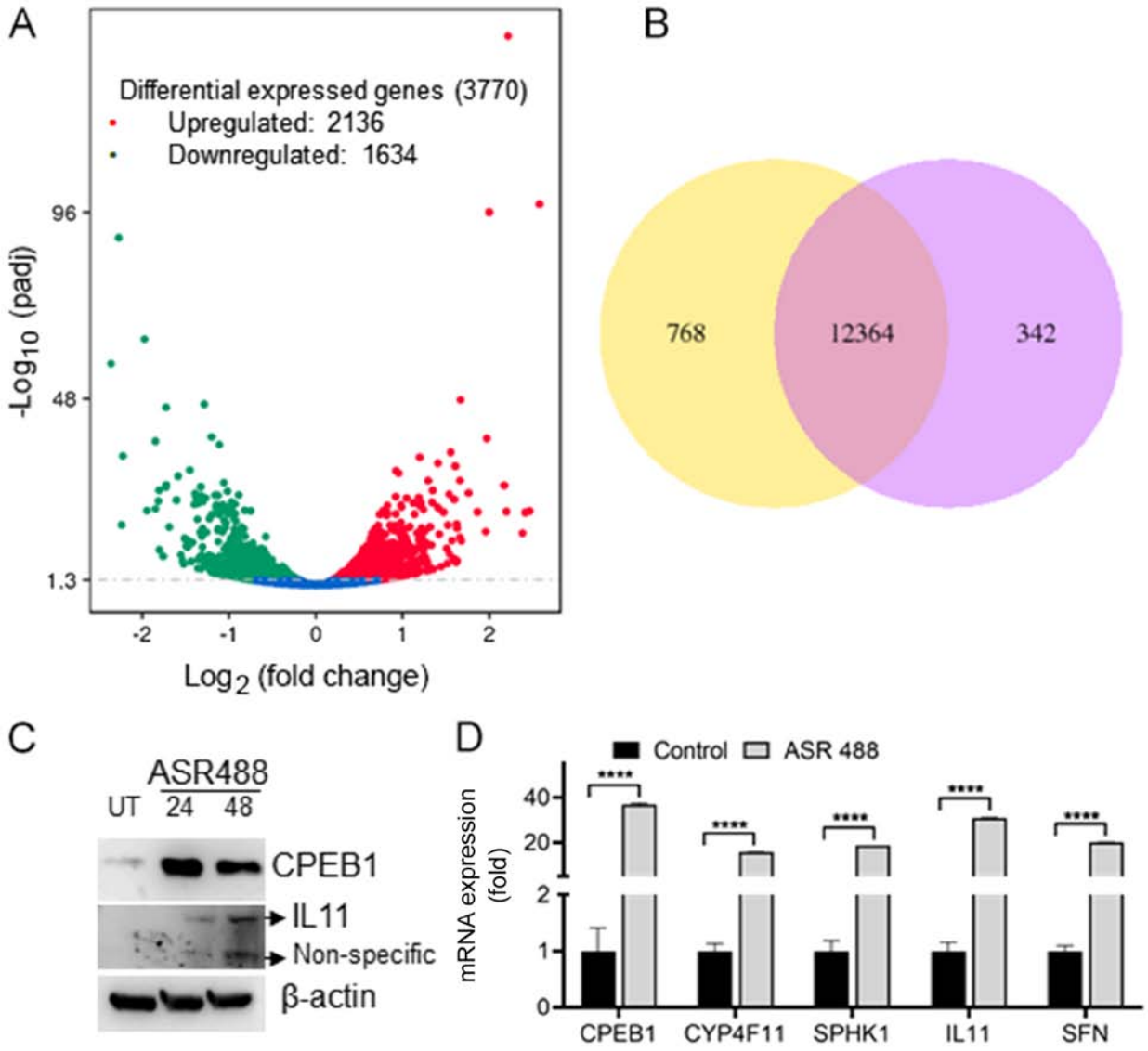

Figure 2. Differential expression of genes in ASR488-treated MIBC cells. (A) Distribution of DEGs demonstrated by Volcano diagram. The upregulated genes in ASR488-treated TCCSUP cells relative to TCCSUP cells treated with vehicle (DMSO) are presented in red, whereas the green dots represent the downregulated genes. The blue dots represent the genes that are without any significant diversity. (B) Venn diagram. The sum of the numbers in each large circle are the total number of genes in ASR488-treated or vehicle-treated TCCSUP cells, and the common genes among the samples are represented in the overlapping part. (C) Vehicle or ASR488-treated TCCSUP cells were subjected to immunoblotting and CPEB1 and IL11 genes were analyzed. (D) Reverse transcription-quantitative PCR analysis of top upregulated genes are displayed as fold difference between vehicle or ASR488-treated TCCSUP cells. Student's t-test was used to identify statistically significant differences between vehicle and treatment at each concentration. ****P<0.0001. MIBC, muscle-invasive bladder cancer; DEGs, differentially expressed genes; IL, interleukin; UT, vehicle (DMSO) treated TCCSUP cells.

dendrogram showed that the gene profile from vehicle-treated BCa cells was distant from that of ASR488-treated TCCSUP cells (Fig. S1). These results confirm that treating metastatic BCa cells with ASR488 leads to differential expression of key genes.

Functional enrichment of DEGs via GO. To further visualize the relationship between genes in ASR488-treated TCCSUP in context of their expression, distinct clusters of genes were extracted and submitted to gene set enrichment analysis. The GO terms as well as pathways that were significantly over-represented among genes were identified from the clusters. The top GO terms (from BP (Biological Process), CC (Cellular Component), and MF (Molecular Function) categories) enriched by the upregulated and downregulated DEGs were identified (Figs. 3 and 4). The results revealed that the downregulated genes were involved in viral defense response, DNA synthesis and repair (BP category, Fig. 3A), transcriptionally active chromatin, endoplasmic reticulum quality (CC Category, Fig. 3B), kinase activity, and DNA polymerase activity (MF category, Fig. 3C). On the other hand, the upregulated genes were mainly associated with regulation of cellular metabolic processes and regulation of ubiquitin-protein ligase activity in the BP category (Fig. 4A). In the CC category, these upregulated genes were involved in the regulation of the proteasome complex, endopeptidase complex, and myelin sheath (Fig. 4B). Whereas, in the MF category, these were mainly involved in cadherin binding, cell molecular adhesion binding, and threonine-type endopeptidase activity (Fig. 4C).

Table I. List of top 10 upregulated genes in ASR488-treated TCCSUP cells.

Gene symbol	Log_2 (fold-change)	P-value
CPEB1	6.3347	$4.17x10^{-3}$
CYP4F11	8.3568	$1.09x10^{-8}$
SPHK1	4.6389	$1.32x10^{-41}$
IL11	2.9265	$8.14x10^{-10}$
SFN	3.7239	$1.54x10^{-9}$
ACTG2	3.0293	$8.70x10^{-12}$
HSPA6	3.5985	$6.27x10^{-9}$
TAGLN	2.3661	$4.54x10^{-8}$
MAP1A	2.1205	$8.78x10^{-7}$
GNGT2	2.5802	$3.62x10^{-6}$

Table II. List of top 10 downregulated genes in ASR488-treated TCCSUP cells.

Gene symbol	Log_2 (fold-change)	P-value
DDX60	-2.5069	$1.59x10^{-8}$
GBP4	-2.2704	$2.98x10^{-8}$
BBOX1	-2.2384	$7.26x10^{-6}$
RSAD2	-2.2235	$9.71x10^{-8}$
OASL	-1.9737	$8.15x10^{-7}$
FOS	-1.9465	$9.91x10^{-5}$
IFIT2	-1.8473	$1.66x10^{-6}$
CMPK2	-1.8470	$8.78x10^{-7}$
STEAP4	-1.8141	$2.70x10^{-5}$
IFI44L	-1.9791	$1.04x10^{-5}$

KEGG pathway analysis of DEGs. To analyze the functional status of DEGs i.e., which DEGs are activated and suppressed in different classes of pathways, the information we got from gene expression analysis of ASR488-treated TCCSUP cells was mapped to the KEGG pathway. Pathway analysis and functional annotation for up- and down-regulated genes were performed. The analysis revealed that 156 up-regulated genes (padj<0.001, log_2 FC>2) and 82 down-regulated genes (padj<0.001, log_2 FC<-2) were mapped to 238 KEGG pathways. The top 20 enriched pathways are displayed in Fig. 5. The results indicate that the DEGs are highly clustered in several signaling pathways, such as focal adhesion, neurotrophin-signaling, and p53 signaling, as well as in protein processing in the endoplasmic reticulum and BCa (Fig. 5B). More interestingly, the down-regulated pathways in ASR488-treated BCa cells were enriched in DEGs involved in DNA replication, mismatch repair, RNA degradation, nucleotide excision repair, TGFβ signaling, and pathways in cancer (Fig. 5C). Downregulation of the DNA replication, mismatch repair, and pathways in cancer make the ASR488 treated TCCSUP cells less proliferative and invasive, finally contributing to the decreased tumorigenic capacity of the cells.

Reactome pathway analysis of DEGs. To further analyze gene sets (pre-defined groups of genes that are functionally related), a reactome enrichment analysis was performed (Fig. 6A). It is well established that consistent perturbations over such gene sets frequently cause mechanistic changes. The results from our study demonstrate that the significantly enriched reactome pathways of upregulated DEGs were related to ornithine decarboxylase regulation, regulation of tumor suppressor RUNX3 expression, and non-canonical NFκB signaling (Fig. 6B). Interestingly, the reactome data indicated that gene sets related to ubiquitin-dependent degradation of cyclin D1 were significantly upregulated, which indicated arrest of the cell cycle in the treatment group and supported the growth inhibitory effect of ASR488 treatment in TCCSUP cells (Fig. 6B). The data also demonstrate significant downregulation of gene networks involved in telomere C strand synthesis and DNA damage checkpoints (Fig. 6C).

Discussion

Among the limited options available to patients with BCa, programmed cell death protein 1 (PD-1) pathway inhibitors are a major category of inhibitors (18,19). However, only a small group of patients respond, and options after disease progression are a significant unmet need. Over 20 small molecule drugs are being successfully used in cancer treatment after being approved for clinical use. Nevertheless, these are not without limitations. Non-specific binding to multiple molecular targets such as cell surface receptors increase the the risk of toxicity (20). It is thus important to screen the promising small molecules for their effect on crucial pathways, which should remain largely unaffected during treatment of BCa. Analysis of complex signaling networks and genes, which are differentially expressed after treatment, can provide valuable input before progressing to further preclinical as well as clinical trials.

We have screened a library of small molecules (analogs of Withaferin A) and observed significant growth inhibition and induction of apoptosis in MIBC cells with ASR488 treatment. To further explore the mechanism of action of ASR488 in regulating the growth of BCa, we analyzed the gene expression profiling using RNA-seq.

We observed that ASR488 treatment significantly affected the expression of key regulatory genes, such as CPEB and IL11. Depletion of CPEB1 expression levels has been explicitly linked with increased metastatic potential in different cancer types (21,22). CPEB1/2 downregulate TWIST1 expression, which is considered one of the main inducers of EMT (23). It is also been shown that skin and lung cells were able to circumvent the M1 crisis stage of senescence in CPEB knockdown cells by undergoing telomere erosion, and its reintroduction restored the senescence-like phenotype. The knockdown was also followed with recommencement of cellular growth and fewer mitochondria. These cells had reduced respiration and reactive oxygen species (ROS) and resembled transformed cells by having normal ATP levels, and enhanced rates of glycolysis (24). We also observed that mitochondrial translational elongation and telomere C strand synthesis was significantly affected in GO and reactome enrichment analysis, respectively. Additionally, CPEB knockdown cells

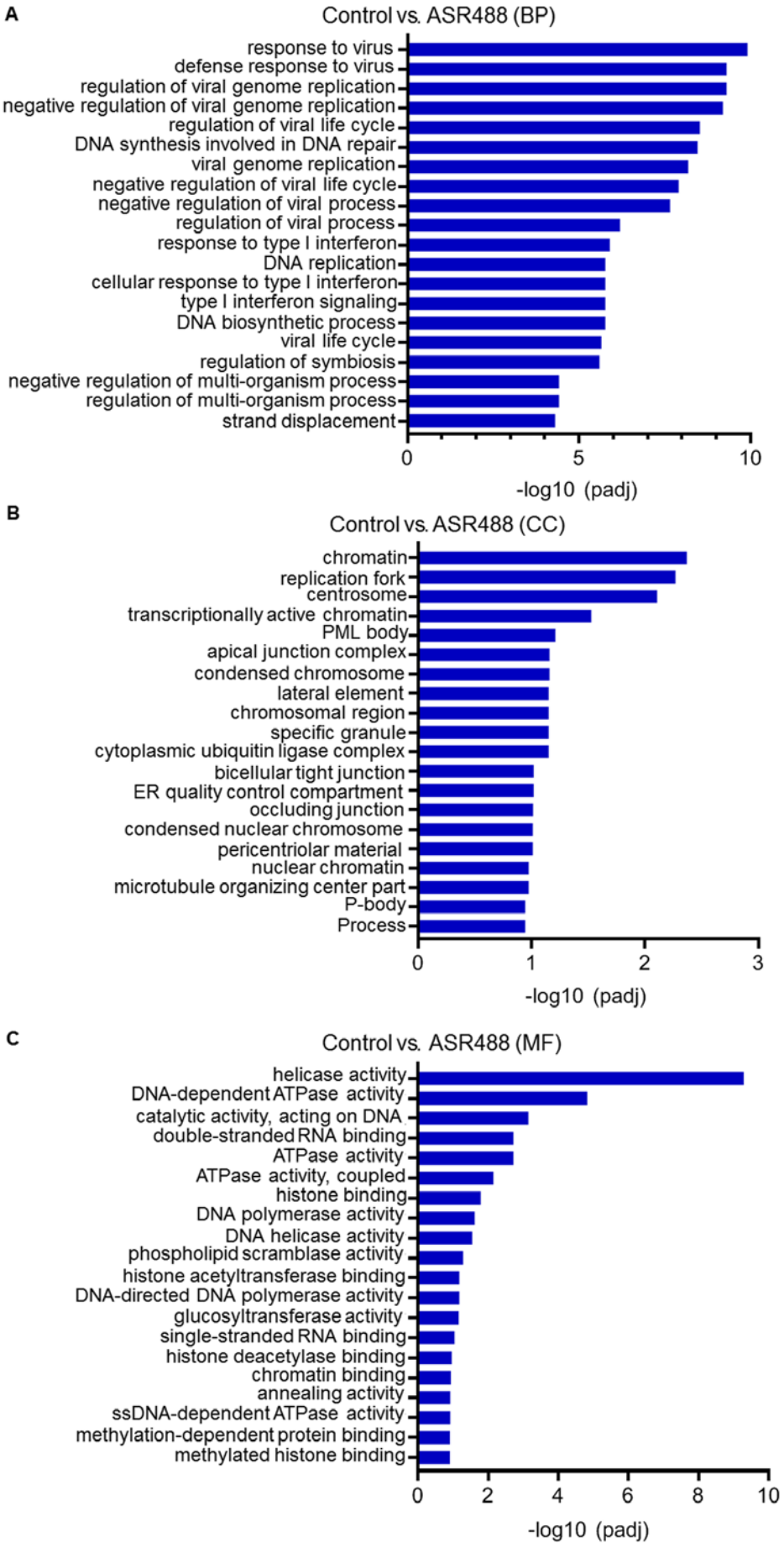

Figure 3. Gene Ontology enrichment analysis. The top 20 downregulated enriched differentially expressed genes were grouped into functional groups, which have been presented as (A) BP, (B) CC and (C) MF. BP, biological process; CC, cellular component; MF, molecular function.

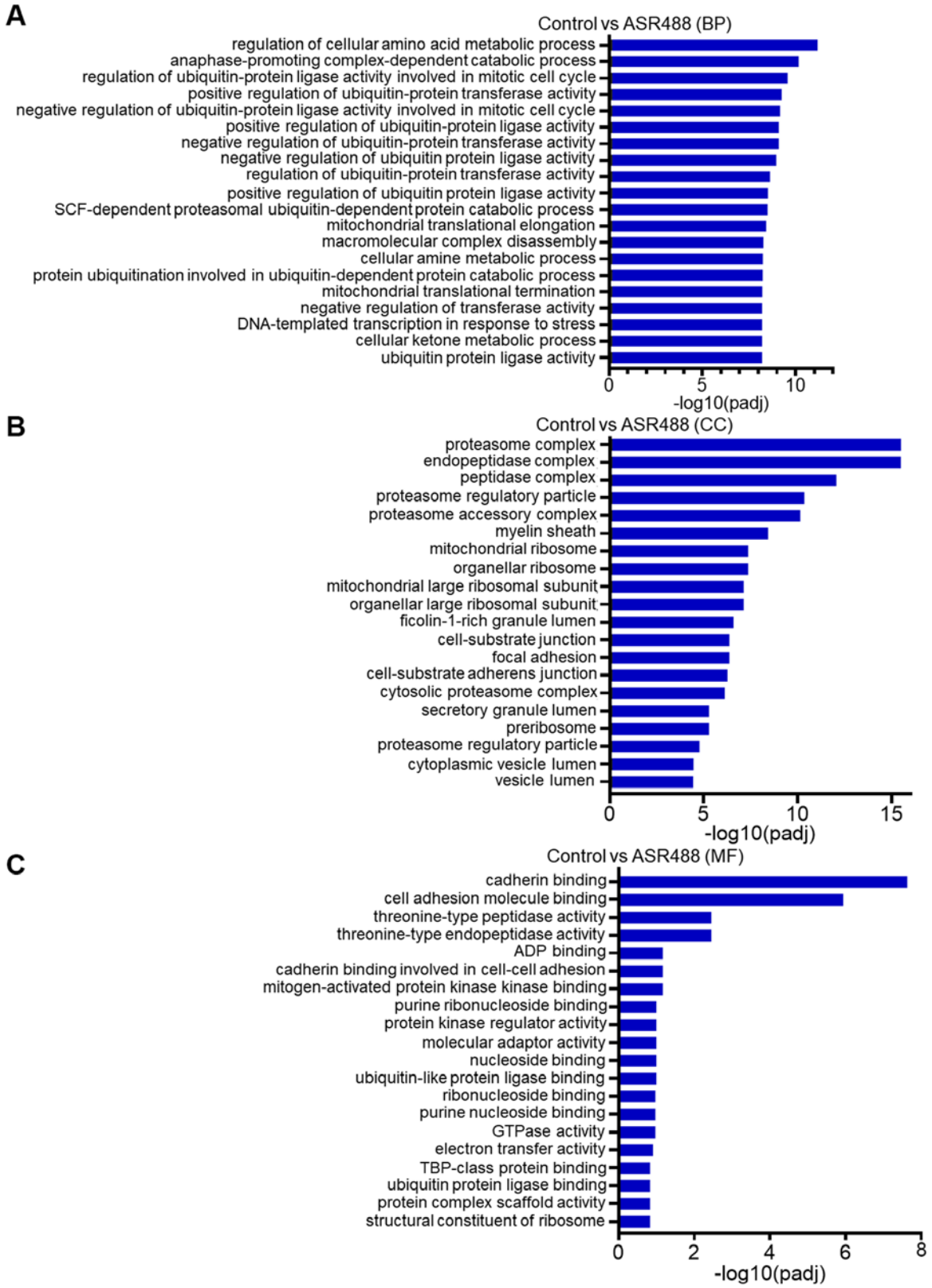

Figure 4. Gene ontology enrichment analysis. The top 20 upregulated enriched differentially expressed genes were grouped into functional groups, which have been presented as (A) BP, (B) CC and (C) MF. BP, biological process; CC, cellular component; MF, molecular function.

have p53 mRNA with an unusually short poly(A) tail, which ultimately resulted in a significant decrease (greater than 50%) in p53 protein levels (24). Our reactome analysis indicates that ASR488 treatment significantly affected p53 stabilization and the p53 dependent DNA damage checkpoint. Overall, these findings indicate that regulation of mitochondrial processes and p53 stabilization might be possible mechanisms for cell growth arrest in ASR488-treated BCa cells.

Another significantly upregulated gene in our study, IL11, has been shown to be dysregulated in human gastric (25),

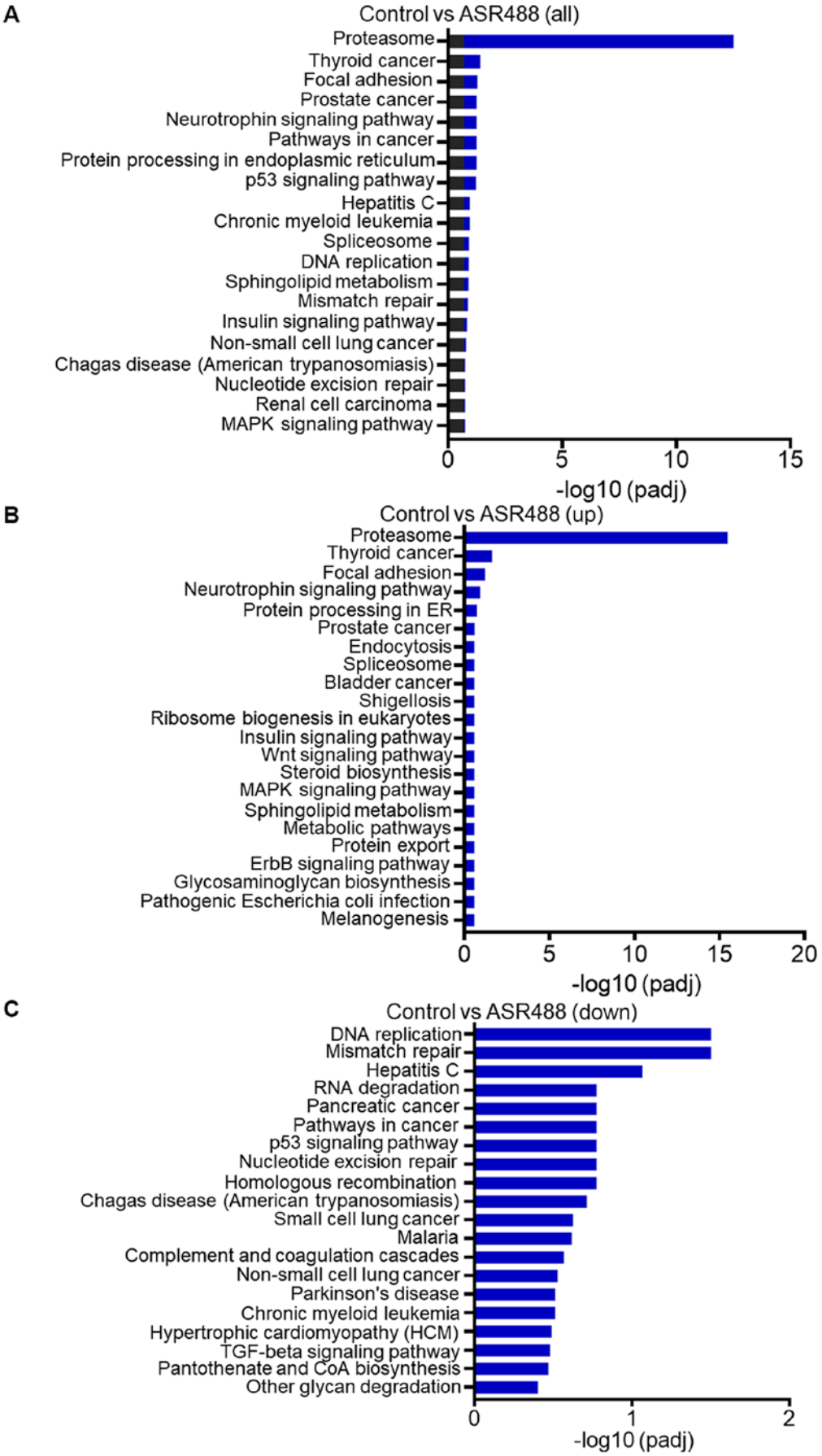

Figure 5. KEGG pathway analysis. Fisher's exact test was used to perform KEGG pathway enrichment analysis. (A) KEGG pathways (P<0.05) that were significantly enriched. Top 20 significantly enriched pathways in the KEGG enrichment analysis results. (B) Top 20 enriched pathways that were significantly upregulated in the KEGG enrichment analysis results. (C) Top 20 significantly downregulated enriched pathways in the KEGG enrichment analysis results. For each KEGG pathway, the fold enrichment of the pathway is indicated by the bar. KEGG, Kyoto Encyclopedia of Genes and Genomes.

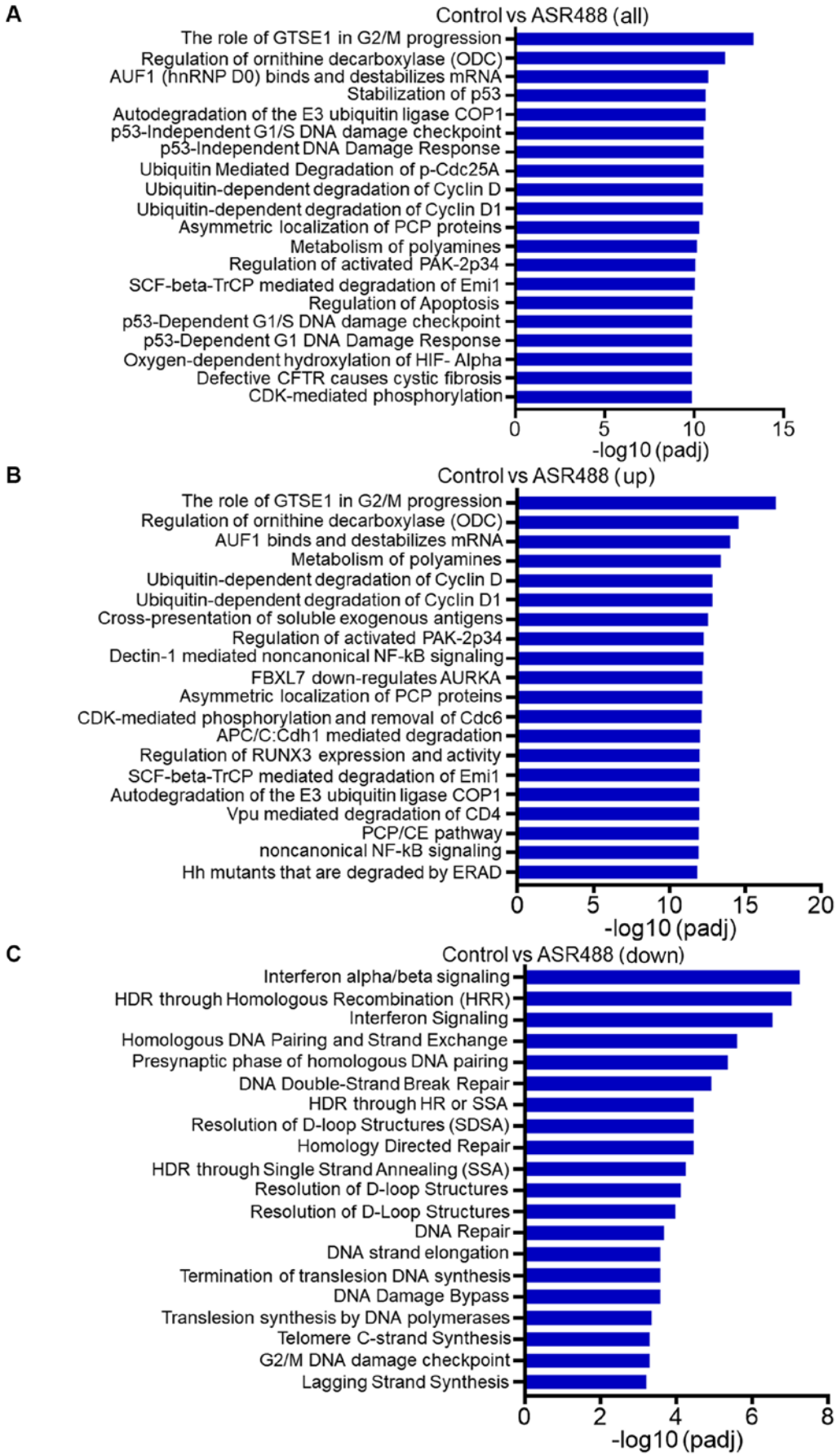

Figure 6. Reactome pathway analysis. The reactome pathway enrichment analysis of differentially expressed genes. Top 20 pathways that were significantly affected are listed. These pathways include both the upregulated and downregulated pathways. (A) Top 20 significantly enriched pathways in the Reactome analysis results. (B) A total of 20 enriched pathways that are significantly upregulated in the Reactome analysis results. (C) Top 20 significantly downregulated enriched in the Reactome analysis results.

colon (26), breast (27), and bladder cancers (28). Unlike IL6, the role of IL-11 in various inflammation-associated cancers is not well studied. Interestingly, IL-11 has generally been considered as an anti-inflammatory cytokine, which is in contrast with the well-studied pro-inflammatory function of IL-6. Although aggressiveness of several cancer types has been attributed to increased IL11 levels, a decrease in IL11 has been specifically recognized as a factor contributing to carcinogenesis of the bladder. Wu *et al* (28) have shown that the expression of IL-11 was downregulated in human BCa cell lines and transitional cell carcinoma (TCC) when it was compared with primary human bladder cell culture. The same study also demonstrated that the BCa patients samples had reduced urinary levels of IL-11 in comparison to healthy subjects (28). In our study, another important signaling immune pathway (the TGFβ pathway) was significantly downregulated in KEGG analysis. It has been demonstrated that levels of EMT markers, such as vimentin, slug, and twist, are downregulated in TGFβ knockout mice, and abrogation of TGFβ pathway depletes tumorigenic and invasive potential in an induced mouse BCa model (1). As discussed in an earlier section, there is also a proven direct link between CPEB expression and downregulation of twist1, CPEB overexpression combined with downregulation of TGFβ signaling during ASR488 treatment could reduce the metastatic potential of BCa cells.

Another interesting observation from the GO enrichment analysis was the significant downregulation of ATPase activity in ASR488-treated BCa cells. ATPase is considered as an important ion transporter that is involved in signal transduction. It is well established that ATPase expression profile is altered in various tumors, such as breast cancer (29). Inhibition of ATPase activity significantly reduced cell proliferation, motility, and invasion in breast cancer. More recently, downregulation of longevity assurance homolog 2 of yeast LAG1 (LASS2) has been associated with a poor prognosis in patients with BCa. LASS2 binds directly to subunit C of vacuolar H^+-ATPase (V-ATPase) and its silencing resulted in increased ATPase activity, which, in turn activated secreted matrix metalloproteinase (MMP)-2 and MMP-9, and thus enhanced cell proliferation, cell survival, and cell invasion *in vitro*, as well as increase of BCa growth rate *in vivo* (30). This decrease in ATP activity is important to point out as we have seen that CPEB knockout results in resumption of cell growth, fewer mitochondria, and resembled transformed cells by maintaining normal ATP levels by increasing glycolysis (24). Hence, with normal ATPase activity or levels, the cells might bypass the M1 crisis stage of senescence and thus act as transformed cells with increased proliferative profile. However, an increased CPEB level and decrease in ATPase activity will be detrimental to the growth of these cancer cells and, ultimately, lead to downregulation of metastatic and proliferative capacities.

In summary, using RNAseq data, here we identify signaling molecules and pathways that are significantly affected upon ASR488 treatment in MIBC cells. Interestingly, these pathways are interlinked in a way that reduces the proliferative and metastatic efficacy of MIBC cells. This study also indicated that ASR488 might be a potential small molecule for BCa treatment. However, these results need to be validated in other *in vitro* and *in vivo* BCa models.

Acknowledgements

Not applicable.

Funding

No funding was received.

Availability of data and materials

The datasets used and/or analyzed during the current study are available from the corresponding author on reasonable request.

Authors' contributions

CD and MA conceived and supervised the study. AT and VK performed the experiments, conducted the analysis as well as the interpretation of the RNASeq data, performed the statistical analysis and wrote the manuscript. BC and US performed the statistical analysis and compiled the data into figures and revised the manuscript. AS conceptualized, designed and performed synthesis of the compound. AS critically revised the manuscript for its intellectual content and also gave final approval for the corrected version of manuscript. All authors have read and approved the final version of the manuscript.

Ethics approval and consent to participate

Not applicable.

Patient consent for publication

Not applicable.

Competing interests

The authors declare that they have no competing interests.

References

1. Liang Y, Zhu F, Zhang H, Chen D, Zhang X, Gao Q and Li Y: Conditional ablation of TGF-β signaling inhibits tumor progression and invasion in an induced mouse bladder cancer model. Sci Rep 6: 29479, 2016.
2. Siegel RL, Miller KD and Jemal A: Cancer statistics, 2018. CA Cancer J Clin 68: 7-30, 2018.
3. Erlich A and Zlotta AR: Treatment of bladder cancer in the elderly. Investig Clin Urol 57 (Suppl 1): S26-S35, 2016.
4. van den Bosch S and Alfred Witjes J: Long-term cancer-specific survival in patients with high-risk, non-muscle-invasive bladder cancer and tumour progression: A systematic review. Eur Urol 60: 493-500, 2011.
5. Pectasides D, Pectasides M and Nikolaou M: Adjuvant and neoadjuvant chemotherapy in muscle invasive bladder cancer: Literature review. Eur Urol 48: 60-68, 2005.
6. Akand M, Kilic Ö, Harmankaya I, Karabagli P, Yavas Ç and Ata Ö: Aggressive treatment for urothelial cancer-complete urinary tract extirpation: Operative feasibility in two cases. Turk J Urol 45: 393-397, 2018.
7. Mathes J, Rausch S, Todenhöfer T and Stenzl A: Trimodal therapy for muscle-invasive bladder cancer. Expert Rev Anticancer Ther 18: 1219-1229, 2018.
8. Roberts JT, von der Maase H, Sengeløv L, Conte PF, Dogliotti L, Oliver T, Moore MJ, Zimmermann A and Arning M: Long-term survival results of a randomized trial comparing gemcitabine/cisplatin and methotrexate/vinblastine/doxorubicin/cisplatin in patients with locally advanced and metastatic bladder cancer. Ann Oncol 17 (Suppl 5): v118-v122, 2006.

9. Padma VV: An overview of targeted cancer therapy. Biomedicine (Taipei) 5: 19, 2015.
10. Carter PJ: Potent antibody therapeutics by design. Nat Rev Immunol 6: 343-357, 2006.
11. Hoelder S, Clarke PA and Workman P: Discovery of small molecule cancer drugs: Successes, challenges and opportunities. Mol Oncol 6: 155-176, 2012.
12. Imai K and Takaoka A: Comparing antibody and small-molecule therapies for cancer. Nat Rev Cancer 6: 714-727, 2006.
13. Mu Y and Sun D: Lapatinib, a dual inhibitor of epidermal growth factor receptor (EGFR) and HER-2, enhances radiosensitivity in mouse bladder tumor Line-2 (MBT-2) cells in vitro and in vivo. Med Sci Monit 24: 5811-5819, 2018.
14. Hänze J, Kessel F, Di Fazio P, Hofmann R and Hegele A: Effects of multi and selective targeted tyrosine kinase inhibitors on function and signaling of different bladder cancer cells. Biomed Pharmacother 106: 316-325, 2018.
15. Yan J, Risacher SL, Shen L and Saykin AJ: Network approaches to systems biology analysis of complex disease: Integrative methods for multi-omics data. Brief Bioinform 19: 1370-1381, 2018.
16. Tyagi A, Chandrasekaran B, Kolluru V, Rai S, Jordan AC, Houda A, Messer J, Ankem M, Damodaran C and Haddad A: Combination of androgen receptor inhibitor and cisplatin, an effective treatment strategy for urothelial carcinoma of the bladder. Urol Oncol 37: 492-502, 2019.
17. Pal D, Tyagi A, Chandrasekaran B, Alattasi H, Ankem MK, Sharma AK and Damodaran C: Suppression of Notch1 and AKT mediated epithelial to mesenchymal transition by Verrucarin J in metastatic colon cancer. Cell Death Dis 9: 798, 2018.
18. Bellmunt J, Powles T and Vogelzang NJ: A review on the evolution of PD-1/PD-L1 immunotherapy for bladder cancer: The future is now. Cancer Treat Rev 54: 58-67, 2017.
19. Sundararajan S and Vogelzang NJ: Anti-PD-1 and PD-L1 therapy for bladder cancer: What is on the horizon? Future Oncol 11: 2299-2306, 2015.
20. Deng J, Peng M, Wang Z, Zhou S, Xiao D, Deng J, Yang X, Peng J and Yang X: Novel application of metformin combined with targeted drugs on anticancer treatment. Cancer Sci 110: 23-30, 2019.
21. Nagaoka K, Fujii K, Zhang H, Usuda K, Watanabe G, Ivshina M and Richter JD: CPEB1 mediates epithelial-to-mesenchyme transition and breast cancer metastasis. Oncogene 35: 2893-2901, 2016.
22. Grudzien-Nogalska E, Reed BC and Rhoads RE: CPEB1 promotes differentiation and suppresses EMT in mammary epithelial cells. J Cell Sci 127: 2326-2338, 2014.
23. Chen Y, Tsai YH and Tseng SH: Regulation of the expression of cytoplasmic polyadenylation element binding proteins for the treatment of cancer. Anticancer Res 36: 5673-5680, 2016.
24. Burns DM and Richter JD: CPEB regulation of human cellular senescence, energy metabolism, and p53 mRNA translation. Genes Dev 22: 3449-3460, 2008.
25. Putoczki TL, Thiem S, Loving A, Busuttil RA, Wilson NJ, Ziegler PK, Nguyen PM, Preaudet A, Farid R, Edwards KM, *et al*: Interleukin-11 is the dominant IL-6 family cytokine during gastrointestinal tumorigenesis and can be targeted therapeutically. Cancer Cell 24: 257-271, 2013.
26. Ernst M and Putoczki TL: Targeting IL-11 signaling in colon cancer. Oncotarget 4: 1860-1861, 2013.
27. Johnstone CN, Chand A, Putoczki TL and Ernst M: Emerging roles for IL-11 signaling in cancer development and progression: Focus on breast cancer. Cytokine Growth Factor Rev 26: 489-498, 2015.
28. Wu D, Tao J, Ding J, Qu P, Lu Q and Zhang W: Interleukin-11, an interleukin-6-like cytokine, is a promising predictor for bladder cancer prognosis. Mol Med Rep 7: 684-688, 2013.
29. Khajah MA, Mathew PM and Luqmani YA: Na^+/K^+ ATPase activity promotes invasion of endocrine resistant breast cancer cells. PLoS One 13: e0193779, 2018.
30. Wang H, Zuo Y, Ding M, Ke C, Yan R, Zhan H, Liu J, Wang W, Li N and Wang J: LASS2 inhibits growth and invasion of bladder cancer by regulating ATPase activity. Oncol Lett 13: 661-668, 2017.